

## Electrothermal microthruster

Cervone, Angelo; Guerrieri, Dadui Cordeiro; Silva, Marsil de Athayde Costa e.; Leverone, Fiona

**DOI**

[10.1016/B978-0-12-819037-1.00003-7](https://doi.org/10.1016/B978-0-12-819037-1.00003-7)

**Publication date**

2022

**Document Version**

Final published version

**Published in**

Space Micropropulsion for Nanosatellites

**Citation (APA)**

Cervone, A., Guerrieri, D. C., Silva, M. D. A. C. E., & Leverone, F. (2022). Electrothermal microthruster. In *Space Micropropulsion for Nanosatellites: Progress, Challenges and Future* (pp. 125-149). Elsevier. <https://doi.org/10.1016/B978-0-12-819037-1.00003-7>

**Important note**

To cite this publication, please use the final published version (if applicable). Please check the document version above.

**Copyright**

Other than for strictly personal use, it is not permitted to download, forward or distribute the text or part of it, without the consent of the author(s) and/or copyright holder(s), unless the work is under an open content license such as Creative Commons.

**Takedown policy**

Please contact us and provide details if you believe this document breaches copyrights. We will remove access to the work immediately and investigate your claim.

***Green Open Access added to TU Delft Institutional Repository***

***'You share, we take care!' - Taverne project***

**<https://www.openaccess.nl/en/you-share-we-take-care>**

Otherwise as indicated in the copyright section: the publisher is the copyright holder of this work and the author uses the Dutch legislation to make this work public.

# Electrothermal microthruster

# 5

**Angelo Cervone, PhD<sup>1</sup>, Dadui Cordeiro Guerrieri, PhD<sup>2</sup>,  
Marsil de Athayde Costa e Silva, PhD<sup>2</sup>, Fiona Leverone, PhD<sup>2</sup>**

<sup>1</sup>Assistant Professor, Aerospace Engineering Faculty, Delft University of Technology, Delft, the Netherlands; <sup>2</sup>Aerospace Engineering Faculty, Delft University of Technology, Delft, the Netherlands

## 5.1 Historical background and principle of operation

Electrothermal propulsion can be seen as an intermediate concept between electrical and chemical propulsion. As schematically shown in Fig. 5.1, the propellant is heated electrically and accelerated thermodynamically, typically in a convergent–divergent nozzle. Propellant heating typically happens by means of a resistance (resistojet) or an electrical discharge (arcjet). For the extremely miniaturized applications that will be discussed in this chapter, resistojets are by far the most commonly used form of electrothermal thrusters.

In principle, any propellant can be used, stored in any phase (liquid, solid, or gaseous); in practice, however, liquid propellants are the most widely used. An alternative to liquid propellants is the so-called *warm gas* thrusters, which are basically cold gas systems allowing for additional (usually limited) heating of the gaseous propellant before being accelerated in the nozzle.

In terms of components and operational characteristics, as schematically illustrated in Fig. 5.1, electrothermal thrusters (and in particular resistojets) are very similar to cold gas thrusters: the propellant is stored in a tank, pressurized (when in the liquid phase) by a pressurant gas, and injected in the heating chamber by opening a thrust valve. A pressure regulator is usually not included, especially in miniaturized versions of this propulsion concept, meaning that it is typically operated blow-down and the pressure (and thrust) provided by the system is decreasing over its lifetime. The specific impulse, although higher than cold gas systems due to the higher temperature of the propellant at the nozzle inlet, is still limited due to the limitations in the available heating power and the maximum achievable temperatures.

Electrothermal thrusters have been employed so far in several space applications, since the 60s of the last century when a resistojet concept is reported to have been used on board of the *Vela* satellites [1]. In a detailed conference paper dating back to 1968, Mickelsen and Isley reported the state of art of resistojet thrusters at that time [2]. Particular emphasis is given in that paper to the TRW single-nozzle resistojet successfully flown in the *Vela III* satellite in 1965. This thruster, operating with gaseous

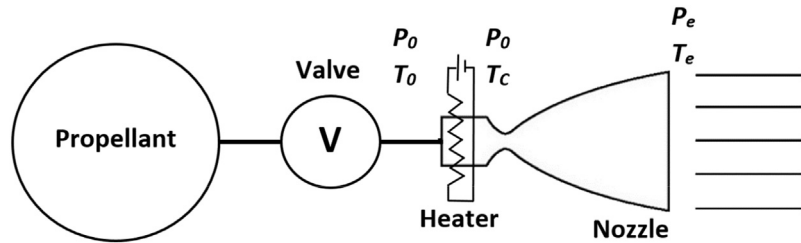


FIGURE 5.1

Schematic of a typical electrothermal propulsion system.

nitrogen, was reported to offer a thrust of approximately 187 mN at a specific impulse of 123 s and an input power of 42 W. A multinozzle version of this resistojet was then successfully flown on the *Advanced Vela* satellite in 1967, with a slightly improved specific impulse of 132 s and a thrust level of 89 mN per nozzle, each requiring a power of 17 W. A different type of resistojet, using liquid ammonia as a propellant, was developed by General Electric and flown on an unspecified NLR spacecraft in 1967. The thrust offered by each nozzle was 44 mN, requiring an input power of 3.2 W. The advantages of using a liquid propellant came at the price of a slight reduction in specific impulse, which was 100 s. Other more advanced electrothermal thruster concepts reported to be under investigation in the 60s included: using miniaturized needle-shaped devices to accelerate and heat the propellant; providing additional heating to the propellant in its supersonic stream in the nozzle; using a radioisotope thermal source to heat the propellant, instead of electrical resistance (the so-called “radioisojet”); or even, in manned spacecraft, using biowaste propellant to feed small resistojet thrusters for drag compensation or attitude control [2].

Despite this large amount of research on the resistojet concept, however, it never became a particularly popular option for use in spacecraft and satellites. Some applications of resistojets in commercial satellites are reported during the 80s of the last century, such as in the first satellites of the INTELSAT-V program. At the present date, Aerojet Rocketdyne offers on the market several electrothermal propulsion options, including both resistojets (MR-501) and arcjets (MR-509, MR-510, MR-512), which have been flown in a number of GEO satellites and in all the Iridium spacecraft. All these options, however, use hydrazine as propellant [3].

The research on miniaturized electrothermal thrusters, on the other hand, is still in its infancy and has not led yet to a significant number of flight-qualified concepts. However, as will be explained in detail in the following sections of this chapter, several universities, companies, and research institutions are conducting extensive research on different types of microresistojet concepts and ideas. The intrinsic simplicity of this propulsion concept, its adaptability to various possible propellants (solid, liquid, or gaseous), and its high thrust-to-power ratio when compared to other electric micropropulsion concepts make it a valid alternative for use in small and very small satellites, especially for the range of thrust in the order of 1–100 mN, which is at the margins of the typically available thrust level of both conventional miniaturized electric and chemical propulsion.

---

## 5.2 Current state of the art of electrothermal micropropulsion

A very good review of the existing electrothermal propulsion concepts is provided by Lemmers [4], to which part of the state of the art presented in this section refers. Other, less conventional options presented in the second part of this section are mainly based on the research performed by the authors of this chapter at the Delft University of Technology. It has to be noted, however, that most of the concepts presented in this section are still at an early stage of development and/or still require flight qualification in orbit. There is therefore still ample margin of development for their performance, effectiveness, and range of potential applications.

### 5.2.1 Conventional microresistojet thrusters

By “conventional” microthruster concepts, we refer here to either the so-called “warm gas” ones, in which a gaseous propellant is heated up (usually in a moderate way) before expelling it in the nozzle, or the vaporizing liquid microresistojets (VLM), where a liquid propellant is heated until vaporization and subsequently expelled in the nozzle.

One of the first warm gas MEMS propulsion modules demonstrated in orbit on a small satellite is the 3U module developed by Nanospace/GOMSpace [5]. This system based on Butane as a propellant, offered a total impulse of 40 Ns and a thrust resolution of 10  $\mu$ N at a power consumption of 2 W, with a wet mass of 350 g and a size of  $10 \times 10 \times 5$  cm<sup>3</sup> (corresponding to half a CubeSat unit). It can be used either as a fully cold gas system, without any heating of the propellant, or in warm gas mode, with slight propellant heating and consequent performance improvement. The full module includes four thrusters each with a thrust of 1 mN, at an operating pressure of 2–5 bar and closed-loop thrust control capabilities ensured by an embedded proportional flow control microvalve. It was demonstrated on the TW-1 satellite constellation, where it was reported to have been successfully used for along-track formation flight, allowing for fine-tuning of the orbital altitude with a control window of 0.5 km.

The CubeSat High Impulse Propulsion System (CHIPS) is a microresistojet system developed by CU Aerospace and VACCO [6,7]. The initial version of this system [6] was making use of the refrigerant gas R134a as propellant, with a specific impulse of 82 s, a thrust level of 30 mN, and a required power of 30 W. A successive version of the system [7], was reported to use R236fa as propellant, with a slightly decreased specific impulse of 68 s, at a thrust level of 20 mN and required power of 25 W. Although its performance is slightly worse than R134a, this alternative propellant (R236fa) was preferred because it allows for lower tank pressure and is compatible with the International Space Station filters, which in turn allows for increased safety in case of deployment from the Station. A peculiar characteristic of this system is that it includes a primary central thruster and four smaller attitude control thrusters. Also, in this case, it is possible to use the system either as a cold

gas or as a resistojet by providing power to a “superheater cartridge,” a small diameter tube in which the propellant flows before reaching the nozzle. By heating the thin walls of this cartridge, it is possible to provide the propellant with the required amount of heating before accelerating it in the nozzle.

A similar type of microresistojet system, but using ammonia as propellant and therefore offering a significantly higher specific impulse, has been developed by Busek Inc. [8]. Also, in this case, the system offers an integrated set of thrusters: a primary one (2–10 mN thrust, with a specific impulse of 150 s) and several, smaller, attitude control ones (0.5 mN thrust, 80 s specific impulse). The rated required power of the system is reported in the range from 3 to 15 W. The system has been laboratory demonstrated also with other propellants (including the refrigerants R134a and R236fa) and is designed to fit into a 1U CubeSat volume. It is claimed to be flight-ready, although no flight demonstration of this system seems to be reported in the open literature.

An interesting self-pressurizing microresistojet option is the RAMPART propulsion system, developed at the University of Arkansas [9] and based on 3D printing manufacturing technologies. The system has a rated thrust level of 500 mN and is designed for use with R134a as propellant. Similar to the previous examples, also in this case the thruster can be used either in a cold gas configuration (with a rated specific impulse of 67 s) or in a warm gas one, where the specific impulse can be increased up to 90 s. In this system, the propellant tank features a MEMS membrane with porous microchannels, that implements the surface tension of the fluid to separate the propellant liquid and gaseous phases. In this way, it is possible to use the vapor pressure of the propellant as a means to pressurize it in the tank, without any need for an additional pressurant gas. The nozzle and its integrated heater, made of several layers of bonded silicon, are based on MEMS manufacturing too.

A particularly interesting water microresistojet system, called AQUARIUS, has been developed by the University of Tokyo for the Japanese deep-space 6U CubeSat EQUULEUS [10]. This system is basically of the VLM type, but includes as particularly innovative feature a prevaporization of the water propellant in a separate vaporization chamber, which allows for complete separation between the thrust chamber and the heating chamber. Although at the cost of increased complexity (as an additional set of valves needs to be installed between the vaporization chamber and the thruster itself), this allows for a significant simplification of the heating process, which does not happen anymore in “real time” during the thrusting maneuver itself, but can be performed in advance in the vaporization chamber, with the actual acceleration of the vaporized propellant happening only after the vaporization is completed. This allows, in turn, for removing most of the fluid dynamics complications coming from the presence of a highly dynamic two-phase flow in the thrust chamber (instabilities, flow oscillations, supersonic collapse of the microbubbles). In addition, a further design feature of this microresistojet system is the use of waste heat from telecommunication components of the satellite as a power source for the vaporization chamber, thus reducing the power need of the system and increasing its intrinsic efficiency.

The AQUARIUS system is based on water stored at ambient pressure and temperature and subsequently heated in the vaporization chamber to 393 K at a pressure of 4 kPa. The nominal thrust is 4 mN, with a rated specific impulse of 70 s and a required power of 20 W. A flight prototype of AQUARIUS has been successfully demonstrated in orbit on the dedicated 3U CubeSat AQT-D, deployed in 2019 from the International Space Station [11].

An interesting alternative application of this concept, currently under research at the University of Tokyo, is in a “dual” configuration where the same water propellant is shared by two different propulsion units: a resistojet based on the same design of AQUARIUS and an ion thruster with a thrust level of 0.25 mN, a specific impulse of 415 s, and a required power of 45 W [12].

As mentioned, the main difference between AQUARIUS and other VLM systems currently under development is the separation between the vaporization and the acceleration processes. Most of the other VLM systems, to the contrary, are based on two-phase vaporizing flow in a heater immediately upstream of the nozzle. This heater can be either “internal” (suspended in the flow and, therefore, directly heating the propellant) or, more frequently, “external”, meaning that it is used to raise the temperature of the whole channel in which the propellant flows and, through the walls of the channel, to heat and eventually vaporize the propellant.

An example of this type of VLM microresistojet is the single-channel thruster developed and manufactured at the Indian Institute of Technology [13,14], Fig. 5.2 (left), which underwent an extensive experimental campaign and demonstrated a thrust of 1 mN using a maximum heater power of 3.6 W with a nozzle throat area of  $130 \times 100 \mu\text{m}$ . This thruster is based on a MEMS silicon chip in which one layer includes the heating channel and the convergent-divergent nozzle, while the layer on the opposite side includes a microheater made of a boron-diffused meanderline resistor in single crystal silicon. Another example is the pulsed microresistojet developed by Tsinghua University [15], Fig. 5.2 (right), working with pulsed heating with an average power of 30 W and generating over 1 s of thrusting a total impulse of 0.2  $\mu\text{Ns}$ . This microresistojet MEMS chip is based on a

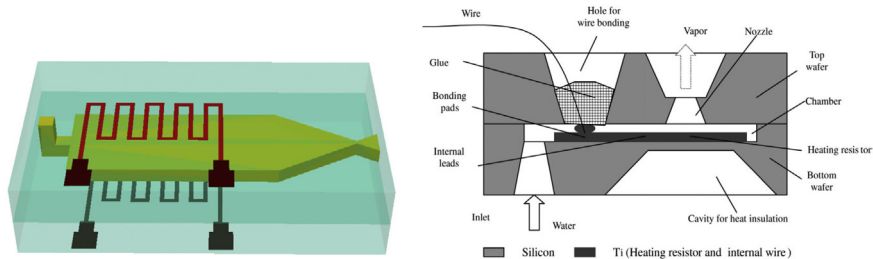


**FIGURE 5.2**

Left: 3D schematic view of the single-channel MEMS resistojet developed at the Indian Institute of Technology [14]. Right: schematic drawing of the MEMS resistojet developed by Tsinghua University [15].

combination of a silicon wafer with metallic Titanium of 200 nm thickness, used for the resistor and the internal wiring. Different from the previous concept, this one is based on an “out-plane” configuration (the propellant inlet and outlet are perpendicular to the silicon wafer) instead of an “in-plane” one (where the propellant inlet and outlet are along the silicon wafer axis). A thrust force ranging from 0.82 to 2.86  $\mu\text{N}$  was experimentally measured for this microresistojet, at a pulse frequency of 30 Hz and a pulse width ranging, respectively, from 500 to 900  $\mu\text{s}$ . Both thrusters shown in Fig. 5.2 use water as propellant.

However, the study and characterization of MEMS microresistojet thrusters date back to the work carried out around the end of the last century at the Jet Propulsion Laboratory of California Institute of Technology [16,17] and at the University of California in Davis [18]. The latter, see Fig. 5.3, proposed in particular two different designs of the microresistojet MEMS chip, an in-plane and an out-plane one. Water was used as propellant for the experimental characterization of the thrusters, achieving a maximum thrust level of approximately 0.19 mN with an input power of 6.7 W. As such, this thruster can be considered as the first laboratory demonstrated microresistojet concept based on MEMS manufacturing technology.

Finally, Delft University of technology is currently developing a MEMS microresistojet system for small satellites using liquid water as a propellant [19,20]. The thruster (Fig. 5.4) is based on a modular approach that allows to manufacture, in the same MEMS wafer, different thrusters based on different combinations of heating channels (either serpentine or diamond shaped) and nozzles. The thruster is heated by metallic molybdenum heaters and designed for a thrust in the range 0.6–1 mN and a specific impulse higher than 100 s, with a chamber pressure in the order of 5 bar. This VLM concept underwent several test campaigns that showed once again the extreme sensitivity of required input power to the chamber pressure, as well as the possibility of using the measured value of the heater resistance as an accurate measurement of the wall temperature in the heating chamber [21].

MEMS and their silicon-based philosophy are not the only options for VLM microresistojets. Some research has been conducted in the past on thrusters based on cofired ceramics, such as those at the National University of Singapore [22] and at Nanyang Technological University [23]. While the former was the first

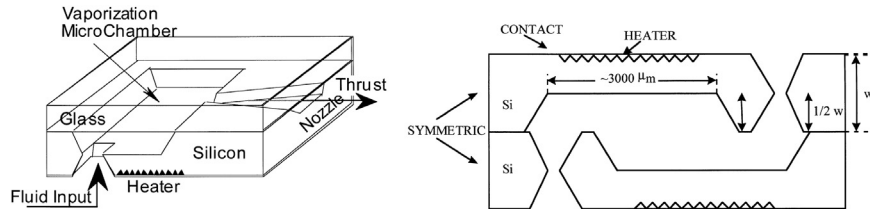


**FIGURE 5.3**

In-plane (left) and out-plane (right) microresistojet configurations proposed by the University of California in Davis [18].



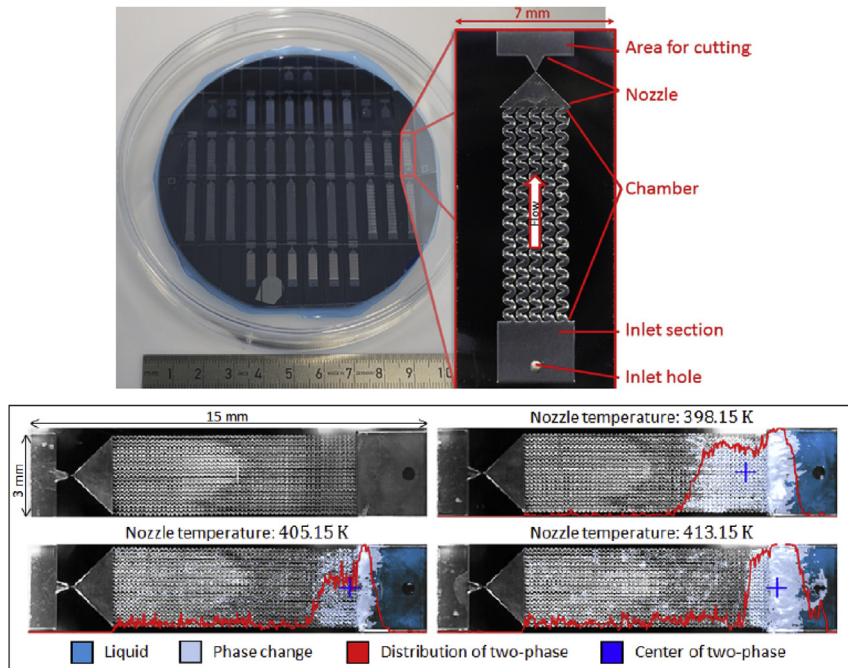


**FIGURE 5.4**

Top: MEMS wafer with different VLM thrusters developed at Delft University of Technology, and one specific thruster based on serpentine heating microchannels [19]. Bottom: vaporizing flow pattern in the thruster at different flow temperatures in the heating chamber [20].

research group to demonstrate the advantages of using this alternative material instead of silicon (in particular, its lower costs and relatively simple fabrication process), the latter further extended the concept by proposing a high-temperature design with a multilayer structure and a platinum heater (Fig. 5.5). The thruster was extensively tested, demonstrating 21% less power consumption compared to a VLM of similar characteristics based on silicon, but showing a particularly low specific impulse of just 31 s at a thrust level of 0.63 mN.

A summary of the VLM microresistojet concepts presented in this chapter is provided in Table 5.1. It includes some general info on each concept, as well as its main performance parameters (thrust, specific impulse, required power level) as reported in the open literature. This survey does not claim to be complete or fully exhaustive, but nevertheless it gives a very good overview of the type of VLM concepts developed so far and the performance level that can be expected from them.

The main technological challenge in VLM microresistojets is the presence of an intrinsically unstable two-phase flow in the heating chamber, which in turn leads to difficulties in controlling the thruster. Another challenge is associated with the need

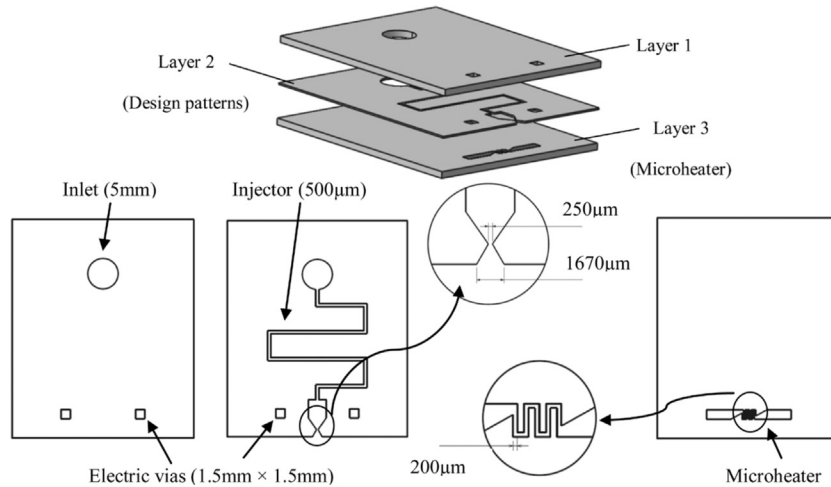


**FIGURE 5.5**

Schematic drawings of the high temperature cofired ceramic VLM proposed by Nanyang Technological University [23].

of using a micronozzle that, as already discussed in [Chapter 3](#) of this book, suffers for significant flow losses when the Reynolds number in the nozzle falls below 1000, a typical situation for microresistojets delivering a thrust in the mN range.

For these reasons, research on the complex fluid dynamics inside the heating and thrust chamber of VLM microresistojets is of fundamental importance for a better design and understanding of these devices. An important contribution to this respect has been given by the research funded by the Taiwan National Applied Research Laboratories [24], which conducted an extensive analysis and experimentation on a VLM with a single channel heating chamber. They were the first to identify a clear relationship in VLM thrusters between mass flow rate, pressure, and heating power (see [Section 5.4](#) for more details): for a given heating power provided to the thruster, the mass flow rate (and thus, the thrust) is a direct function of the pressure in the heating chamber. This means that, when pressure oscillations are present (e.g., due to instabilities caused by the two-phase flow), they generate in turn thrust oscillations, if the input power is kept constant, or as an alternative require to continuously control the input power as a function of the pressure, if the desired outcome is to keep stable thrust level. The flow visualization presented in Ref. [24] also led to the identification of four different flow patterns in the thruster, each with its own characteristics, depending on the mass flow rate, pressure, and channel geometry. This research was further extended by the Chinese Academy of Sciences [25], with an experimental campaign focused on a VLM with multiple parallel straight channels, which allowed to characterize several possible flow phenomena at the thruster microscale, such as presence of liquid droplets in the nozzle in case of insufficient heating, generation of vapor halos around small irregularities in the thruster,

**Table 5.1** Overview of the VLM microresistojet concepts presented in this chapter (gray rows: options commercially available and/or flight qualified; white rows: options at prototype level).

Name	Developer (propellant)	Thrust [mN]	Isp [s]	Power [W]	Notes
Single-nozzle microresistojet	TRW (nitrogen)	187	123	42	Flown on the Vela III satellite
Multinozzle microresistojet	TRW (nitrogen)	89	132	17	Flown on the advanced vela satellite
Microresistojet	General electric (ammonia)	44	100	3.2	Flown on NLR spacecraft
MR-501	Aerojet rocketdyne (hydrazine)	370	303	493	Flown on BSAT-2 satellite
3U CubeSat propulsion module	NanoSpace/ GOMSpace (Butane)	1	n/a	2	Flown on the TW-1 satellite constellation. Also useable as cold gas.
CHIPS	CU Aerospace/ VACCO (R236fa)	20	68	30	Also useable as cold gas
Microresistojet system	Busek Inc. (ammonia)	0.5–20	80–150	3–15	Includes attitude control thrusters
RAMPART	Univ. Arkansas (R134a)	500	90	n/a	Manufacturing by 3D printing. Also useable as cold gas.
AQUARIUS	Univ. Tokyo (water)	4	70	20	Flown on the AQT-D CubeSat
Single-channel MEMS resistojet	Indian Inst. Technology (water)	1	n/a	3.6	Silicon chip with single heating channel
Pulsed MEMS resistojet	Tsinghua University (water)	0.8–2.9 ( $\cdot 10^{-3}$ )	n/a	30	Designed for pulsed-mode operation
MEMS resistojet	Univ. California Davis (water)	0.19	n/a	6.7	First demonstrated MEMS resistojet ever
VLM MEMS resistojet	TU Delft (Water)	0.6–1	>100	n/a	Modular design, multiple parallel heating channels
Cofired ceramic VLM	Nanyang Technological University (Water)	0.63	31	n/a	Multilayer structure with platinum heater

gradual growth (in some cases degenerating into explosion) of large liquid droplets or even, when input power is excessively high, explosive boiling (Fig. 5.6). All these phenomena typically lead to significant pressure oscillations, which in turn make the controllability of the thruster more difficult.

The above considerations clarify the importance of modeling in an accurate way the flow inside VLM microresistojets, to promptly identify already in the early design phase any possible risks related to flow oscillations and instabilities. Particularly outstanding in this respect is the work conducted at the University of Salento [26,27], especially when looking at the relative simplicity of the models they proposed as compared to their predictive capabilities. The one-dimensional model presented in Ref. [26] is based on a coupled analysis of the steady-state flow in the heating chamber with the nonideal flow in the micronozzle, characterized by adding to the ideal rocket theory equations a semiempirical formula for the estimation of the discharge coefficient in presence of viscous losses. The results, obtained for the thrust and specific impulse of a VLM with multichannel heating chamber and parallel straight channels, showed agreement with the experiments with a relative error significantly lower than 10%.

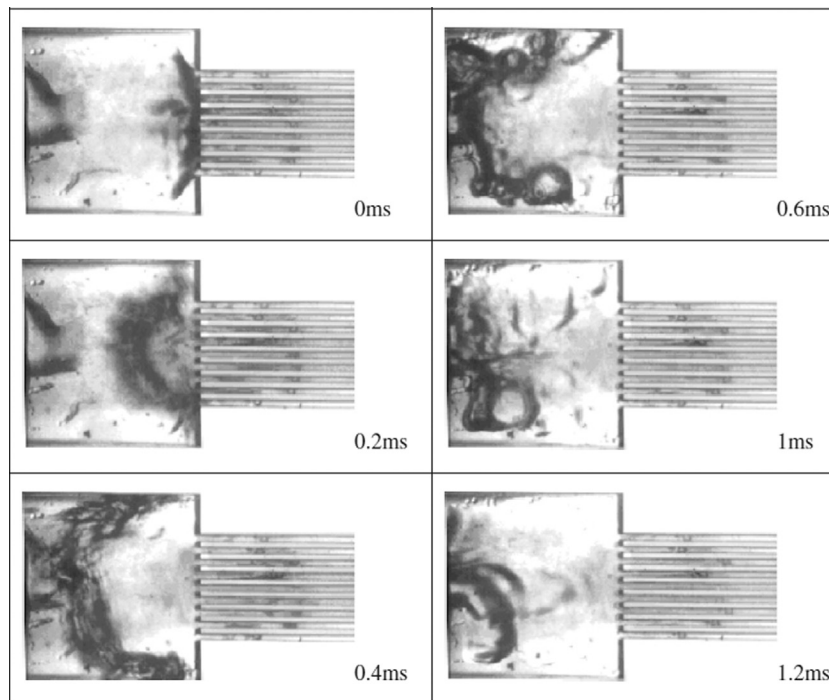


**FIGURE 5.6**

Optical visualization of explosive boiling in the inlet chamber of a VLM with parallel straight heating channels, caused by excessive input power to the thruster. The width of the inlet chamber is 2 mm, while the width of each microchannel is 80  $\mu\text{m}$  [25].

### 5.2.2 A less conventional option: low-pressure microresistojet thrusters

As already mentioned, one of the main issues of miniaturized VLM microresistojets is the use of a micronozzle, which is intrinsically associated with significant flow losses when the Reynolds number becomes particularly low. One way to circumvent this specific issue is by operating the microresistojet at very low pressure, in such a way to work in the rarefied or transitional flow regime. This concept, known in the literature as free molecular microresistojet (FMMR) or more recently low-pressure microresistojet (LPM), allows for completely removing the conventional convergent-divergent nozzle and accelerating propellant particles from a low-pressure plenum only by means of collisions with the high-temperature walls of an expansion slot. Another advantage of this concept is that it allows for dual use, either as microresistojet or cold gas thruster, as it can also operate with no heating of the expansion slot walls.

The FMMR idea was first introduced and researched in the early 2000s by the Air Force Research Laboratory and the University of Southern California [28–31]. Their concept was initially based on a setting in which the heating surface is separated from the expansion slot (Fig. 5.7, left), subsequently improved into a geometry in which the walls of the expansion slots also act as heating surfaces (Fig. 5.7, right). Initial testing of this concept was performed with various candidate propellants (Helium, Nitrogen, Argon, Carbon Dioxide) and plenum pressure ranging from 50 to 300 Pa, demonstrating a thrust level in the range from 0.1 to 1.6 mN and a specific impulse in the range from 40 to 140 s with heater walls temperatures from 325 to 525 K. The same concept was successively demonstrated with water vapor, providing a thrust level of 0.13 mN at a specific impulse of 79 s [32].

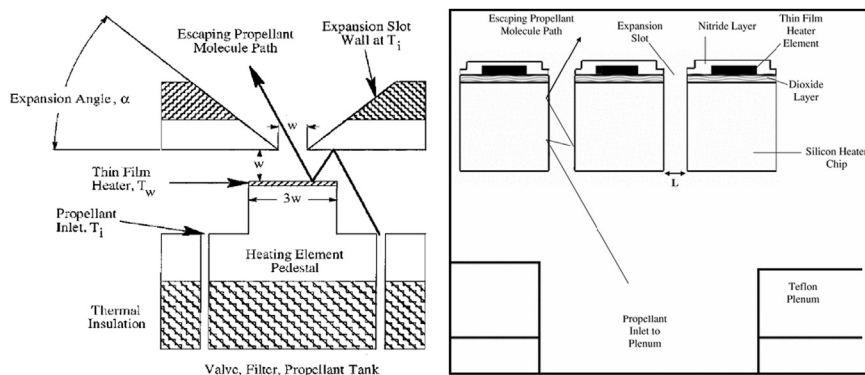


**FIGURE 5.7**

Left: the initial FMMR concept proposed by the Air Force Research Laboratory, with separated heating and expansion surfaces [29]. Right: the improved FMMR concept, using the expansion slot walls as heating surface [30].

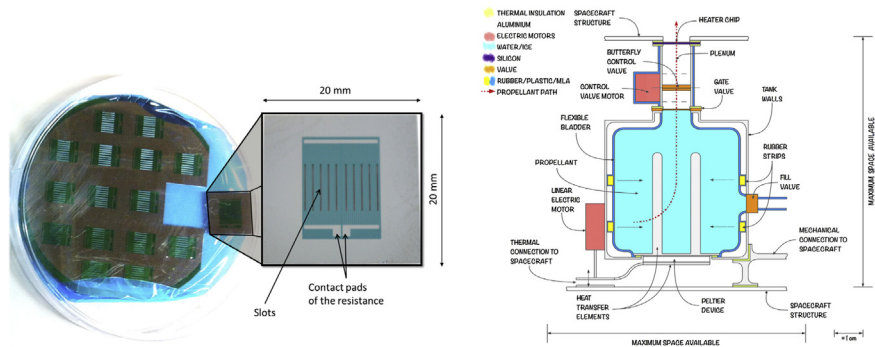


**FIGURE 5.8**

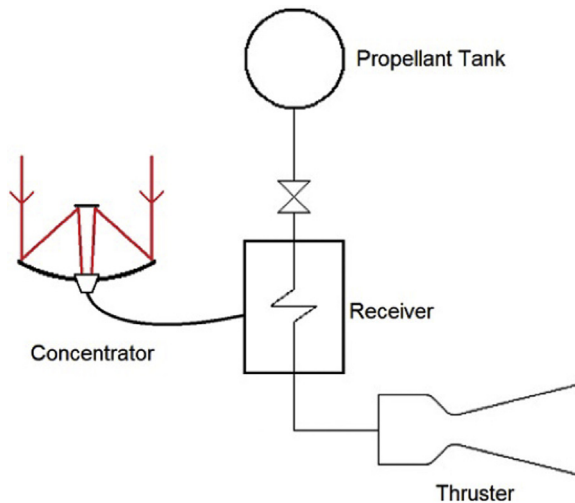
Left: MEMS wafer with different LPM thruster chips developed at Delft University of Technology, and one specific thruster chip based on rectangular expansion slots [33]. Right: sketch of a sublimating ice propulsion system based on the LPM concept [35].

The LPM concept has recently been brought into new life by the research conducted at Delft University of Technology [33–35], where an improved design of this type of microresistojet has been proposed, analyzed, and tested. This concept, intended to work with water vapor as propellant, is based on a MEMS thruster chip heated by molybdenum heaters, with different options, either rectangular or circular, for the geometry of the expansion slots (Fig. 5.8, left). The concept has been extensively tested and demonstrated a thrust in the range from 0.2 to 1.4 mN and a specific impulse in the range from 15 to 40 s, with the heater chip temperature varying from ambient to 149°C and the plenum pressure varying from 200 to 400 Pa.

This concept has also been proposed for use in combination with water stored in the solid state (ice) at a pressure below its triple point, to directly sublimate into vapor (Fig. 5.8, right). The idea is very promising, as it allows to combine the advantages of storing the propellant in the solid phase, with those coming from accelerating a rarefied gas in the thrust chamber. However, for this to become a feasible option, several challenges have to be solved, including in particular how to keep the propellant frozen from launch to actual operation in orbit.

### 5.2.3 An even less conventional option: solar thermal propulsion

Solar thermal propulsion (STP) is an alternative type of electrothermal propulsion in which a concentrator, such as a mirror or a lens, is used to focus sunlight either directly into the propellant or into a heat exchanger, or receiver (Fig. 5.9). Fiber optic cables can be used to transmit the concentrated solar energy from the concentrator to the receiver. Given the significant energy density available from solar thermal sources, propellant temperature can in principle be increased in this kind of system up to values in the order of 3000 K; however, the receiver can also act as energy storage system (based for example on phase change materials) to release this big amount of energy more gradually and allow for slightly lower propellant temperatures.

**FIGURE 5.9**

Schematic of a typical solar thermal propulsion system [36].

STP systems have recently been proposed also for smaller-scale applications, starting from the early 2000s, thanks to the technological advancements in the fields of fiber optics and thermal energy storage, as well as the possibility of employing them in bimodal integrated propulsion and power systems [36]. There are several current challenges to make these miniaturized STP systems actually available to space applications, related to both the concentrator and the receiver technology. For the concentrator, there is a need for more efficient, lightweight, and small optical devices with good optical efficiency, controllability, and deployment capability. For the receiver, the main problems still to be solved are related to insufficient sealing and lifetime of thermal cycling, as well as liquid containment issues. Finally, lightweight insulation materials are necessary to minimize the transfer of heat to other sensitive components of the spacecraft.

The available experimental results for miniaturized STP systems show that it is possible to achieve a thrust level in the order of 1 N at a chamber pressure of 2 bar, operating with a propellant temperature higher than 2000 K by using high-temperature materials such as graphite or rhenium [37,38].

### 5.3 Selection of propellant for electrothermal microthrusters

As previously indicated, one of the main advantages of electrothermal propulsion is that it allows for using virtually any propellant, as the only need is to provide heat to the propellant and eventually vaporize it. However, except for some specific cases

(like the non-conventional idea of using sublimating ice in LPM thrusters, described in Section 5.2), it is preferable to use a propellant that can be stored in liquid state and, therefore, with sufficiently high density without requiring extreme pressurization as it would be the case for propellants stored in the gaseous state.

A detailed analysis of the possible propellant choices for microresistojets has been conducted by the authors of this chapter in Ref. [39]. A total of 95 different propellants were analyzed and prioritized, for both the VLM and LPM cases. As a first step, only propellants that can be stored as liquids (or solids) at ambient temperature, and pressure not higher than 10 bar, were taken into account. This left 63 candidate propellants, which were then ranked based on safety (flammability, instability, and health hazard), performance (specific impulse), and density. These criteria were given weights through a Pugh matrix process, based on the opinion expressed by experts on their relative importance. The final ranking is shown in Fig. 5.10, where not only the average scores are shown (based on the average weight of each criterion among all experts), but also their statistical deviations. More specifically, the middle red line of each box in the figure is the median score, the upper and lower borders of the boxes are the upper and lower quartile, the top and bottom lines are the maximum and minimum value, and the crosses are the outliers. It is clear from these results that nine fluids always score higher than the other ones, irrespectively on the specific expert opinion taken into account for the weighting of the criteria: acetone, ammonia, butane, cyclopropane, ethanol, isobutane, methanol, propene, and water.

These final nine propellants were then evaluated using, as baseline calculation case, the design and requirements of the VLM and LPM devices developed at the

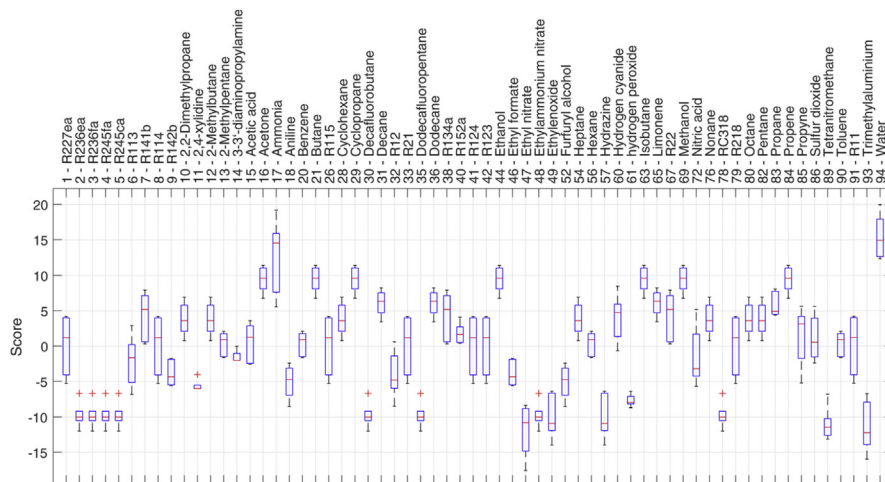


FIGURE 5.10

Global ranking of 63 candidate propellants for microresistojet thrusters, based on criteria weighted by means of a Pugh matrix process [39].



Delft University of Technology. Nevertheless, the results of this analysis (shown in Figs. 5.11 and 5.12) can be considered general and would apply to other designs as well, at least in terms of relative comparison between the propellants.

For each propellant, the theoretical specific impulse and the available Delta-V per unit volume of propellant were calculated, as functions of the required input power, for the full range of temperatures and pressures allowed by the requirements of the baseline thrusters. The performance parameters were calculated based on ideal simplified equations, similar to those presented in Section 5.4 of this chapter.

The results clearly show two best performing propellants: ammonia and water. The higher specific impulse of these propellants is mainly a consequence of their

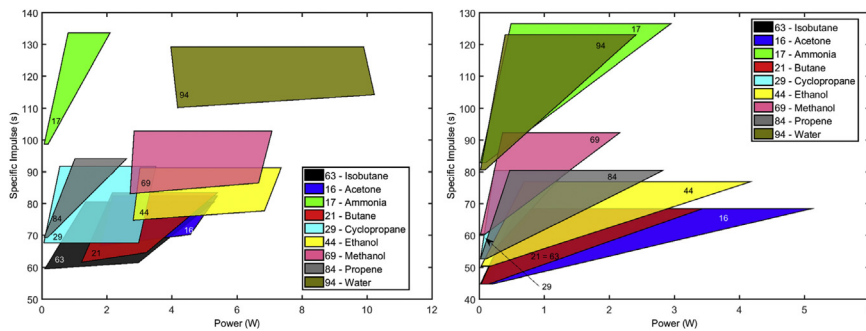


FIGURE 5.11

Specific impulse as a function of the input heating power for the nine best-ranked propellants, for the VLM (left) and LPM (right) case, in the range of pressures and temperatures allowed by the design and requirements of the devices developed at Delft University of Technology [39].

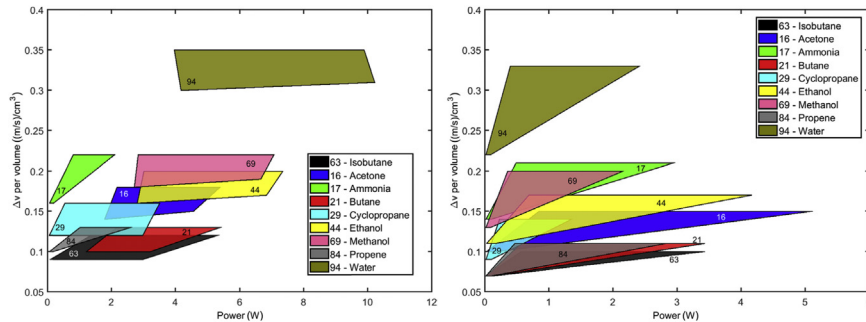


FIGURE 5.12

Delta-V per unit volume of propellant as a function of the input heating power for the nine best-ranked propellants, for the VLM (left) and LPM (right) case, in the range of pressures and temperatures allowed by the design and requirements of the devices developed at Delft University of Technology [39].

lower molecular mass, which allows for accelerating the lighter molecules of propellant at faster velocity with the same amount of energy. However, water suffers for a high value of the latent heat of vaporization, which in the VLM reflects a higher amount of required input power. This issue is not present in the case of the LPM concept, where the propellant is injected in the thruster already in the gaseous state and therefore does not need to be vaporized by the same heaters that are used to accelerate the molecules of propellant in the expansion slots. However, among these two propellants, water clearly shows a higher Delta-V per unit volume, in both the VLM and LPM cases, thanks to its higher liquid density. Therefore, especially for applications in which volume constraints are as important, if not even more important, than mass ones (as it often happens in small satellites and CubeSats), water is probably the best compromise between safety, performance, mass, and volume constraints.

A similar analysis has been conducted in Ref. [36] for STP systems, although for a more limited number of options (water, hydrogen, ammonia). The analysis considered in this case a realistic range of temperatures (1000–2500 K) and thrust levels (0.5 mN–2 N) for a typical STP system, with a nozzle expansion ratio of 100 and a chamber pressure of 2 bar.

The results are in this case less decisive, showing a completely different winner depending on whether the parameter of interest is the specific impulse or the Delta-V per unit volume (see Fig. 5.13). Given its very low molecular mass, hydrogen is clearly the most favorable option in terms of specific impulse, but at the same time shows very poor performance in terms of Delta-V per unit volume. More realistic alternatives in terms of Delta-V per unit volume are represented by ammonia and water, for which similar considerations as the VLM case apply: also, in this case, water seems to represent the best compromise choice between all possible selection criteria.

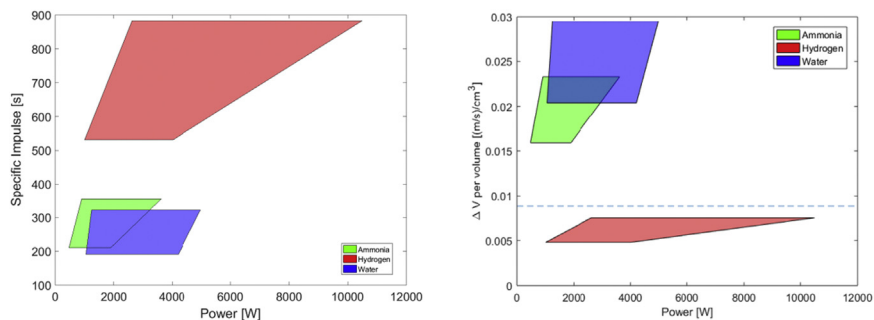


**FIGURE 5.13**

Specific impulse (left) and Delta-V per unit volume of propellant (right) as functions of the input heating power for three potential propellants, for the typical range of pressures and temperatures of a STP system [36].

## 5.4 Theoretical analysis of conventional microresistojets

Since VLM resistojets are typically based on accelerating the propellant in a conventional convergent-divergent nozzle, their performance can be analyzed in a simplified way by applying the ideal rocket theory equations. The assumptions on which these equations are based have already been introduced in [Chapter 3](#) and can be summarized as follows:

- The fluid flowing in the nozzle is a perfect, calorically ideal gas of constant homogeneous chemical composition;
- Flow is steady, isentropic, mono-dimensional, with purely axial velocity;
- No friction or other external forces act on the gas flowing in the nozzle.

The nozzle is convergent–divergent, with an inlet section in which the flow is considered under stagnation conditions (negligible velocity), the throat section where the flow is sonic, and the exhaust section where the flow is typically highly supersonic.

Despite the large number of assumptions and simplifications on which it is based, the ideal rocket theory is still surprisingly accurate in evaluating the performance of the nozzle, with results that normally stay within 10%–15% from the actual values.

With reference to the schematic of [Fig. 5.1](#), we assume that the liquid propellant enters the heating chamber at temperature  $T_0$  and pressure  $p_0$ . The propellant is then heated up to higher temperature  $T_C$  (at which it is in the gaseous state), while it is assumed that no pressure drop takes place in the heating chamber, thus the pressure stays equal to  $p_0$ . The flow is then accelerated in the nozzle, being expelled from it at pressure  $p_e$ , temperature  $T_e$ , and jet velocity  $v_e$ .

Under the ideal rocket theory assumptions, it is possible to derive the following equation for the jet velocity:

$$v_e = \sqrt{\frac{2\gamma}{\gamma - 1} \cdot \frac{R_A}{M_W} \cdot T_C \cdot \left[ 1 - \left( \frac{p_e}{p_0} \right)^{\frac{\gamma-1}{\gamma}} \right]} \quad (5.1)$$

where  $R_A$  is the universal gas constant ( $= 8314 \text{ J/K} \times \text{kmol}$ ),  $M_W$  and  $\gamma$  are the molecular mass and specific heat ratio of the gas flowing in the nozzle.

[Eq. \(5.1\)](#) shows that higher jet velocity can be achieved by selecting a propellant that allows for higher heating temperature and lower molecular mass of the gas flowing in the nozzle (which, in chemical engines, is a mix of the products of the chemical reaction in the chamber).

For the mass flow rate  $\dot{m}$ , the following equation holds:

$$\dot{m} = \frac{p_0 \cdot A^*}{\sqrt{\frac{R_A}{M_W} \cdot T_C}} \cdot \sqrt{\gamma \cdot \left( \frac{1 + \gamma}{2} \right)^{\frac{1+\gamma}{1-\gamma}}} \quad (5.2)$$

where  $A^*$  is the nozzle throat area.

The thrust  $F_T$  produced by a propulsion system, as already mentioned in the previous chapters, can be calculated using the following equation:

$$F_T = \dot{m} \cdot v_e + (p_e - p_a) \cdot A_e = \dot{m} \cdot v_{eq} \quad (5.3)$$

where  $p_a$  is the external ambient pressure and  $A_e$  is the propellant exhaust area. Eq. (5.3) shows that the thrust is made of two different contributions: a “momentum term” (actual momentum exchange between propellant and spacecraft), and a “pressure term” (difference in pressure between the expelled propellant and the external ambient). To write the thrust equation in a more compact way, an *equivalent jet velocity* is usually defined, indicated by  $v_{eq}$  in Eq. (5.3), which accounts for both the momentum and pressure terms in the equation.

The specific impulse is defined as the ratio of the total impulse generated by the engine (thrust integrated over the burn time), to the total weight of propellant used to generate it. It is typically measured in seconds and gives a measure of the propellant consumption efficiency of the system: higher specific impulse means that higher total impulse is generated with the same propellant mass (or, alternatively, the same total impulse can be obtained by using less propellant). If the equivalent jet velocity is constant over time, the specific impulse  $I_{sp}$  can be simply written as follows:

$$I_{sp} = \frac{v_{eq}}{g_0} = \frac{F_T}{\dot{m}g_0} \quad (5.4)$$

where  $g_0$  is always the gravitational acceleration on Earth at sea level ( $= 9.81 \text{ m/s}^2$ ), regardless of the place where the rocket or spacecraft is flying.

Finally, the Delta-V (ideal velocity change experienced by the spacecraft in which the propulsion system is installed, when a given mass of propellant has been expelled) is usually calculated by means of the *rocket equation*:

$$\Delta v = v_{eq} \cdot \ln\left(\frac{M_0}{M_0 - M_P}\right) \quad (5.5)$$

The rocket equation gives the velocity change of a spacecraft with initial mass  $M_0$ , when a mass  $M_P$  of propellant is expelled by its propulsion system with given equivalent jet velocity. However, this is only true under a number of assumptions: no external forces acting on the spacecraft (such as gravity or atmospheric drag); equivalent jet velocity constant over time; propellant expelled in a direction exactly opposite to the flight direction. When at least one of these assumptions is not met, the Delta-V calculated by means of the rocket equation is no longer the actual velocity change of the spacecraft; however, it is still a good indicator of the energy transferred by the propulsion system to the spacecraft, although only part of this energy actually contributes to increasing the actual kinetic energy of the spacecraft.

In a VLM system, Eq. (5.2) for the mass flow rate has to be combined with the following relationship that characterizes the vaporization and heating of the liquid propellant:

$$P_h = \dot{m} \cdot [c_{pL} \cdot (T_{boil} - T_0) + L_h + c_{pG} \cdot (T_C - T_{boil})] \quad (5.6)$$

where  $P_h$  is the available heating power,  $T_{boil}$  is the propellant boiling temperature (which in turn is a function of the heating chamber pressure  $p_0$ ),  $L_h$  is the latent heat of vaporization of the propellant.  $c_{pL}$  and  $c_{pG}$  are the constant pressure specific heat of respectively the liquid and gaseous propellant phase, both are usually functions of the temperature; however, in a simplified model, they can be considered constant and equal to their average value in the relevant range of temperatures. Combining Eqs. (5.2) and (5.6), it is possible to write the following relationship:

$$P_h = \frac{p_0 \cdot A^*}{\sqrt{\frac{R_A}{M_W} \cdot T_C}} \cdot \sqrt{\gamma \cdot \left(\frac{1 + \gamma}{2}\right)^{\frac{1+\gamma}{1-\gamma}}} \cdot [c_{pL} \cdot (T_{boil} - T_0) + L_h + c_{pG} \cdot (T_C - T_{boil})] \quad (5.7)$$

Eq. (5.7), despite having been obtained from an extremely simplified theory, clearly shows the direct relationship not only between heating power and chamber temperature (as expected), but also between heating power and propellant pressure. Although this result has been obtained starting from the ideal rocket theory equations and, therefore, with no flow losses involved, it can be considered of general validity also when losses are present. It confirms that, given a desired temperature at which the propellant has to be heated, the required heating power to achieve that temperature will be a function of the propellant pressure and, therefore, in a system without a pressure regulator it will vary over the lifetime of the system. Furthermore, pressure oscillations and flow instabilities like those typically observed in two-phase boiling flow, previously mentioned in Section 5.2, directly result in the need of controlling the heating power accordingly. This complicates the design of the control electronics and, at the same time, poses additional limitations on the achievable thrust and specific impulse levels.

The modeling equations for LPM microresistojets are significantly different, due to the rarefied flow conditions in this particular concept that make the ideal rocket theory (based on the assumption of continuum flow) not applicable. A simplified set of modeling equations is proposed in Ref. [40] and shortly summarized in the following.

The equations of this model are based on assuming thermodynamic equilibrium inside the LPM plenum and are obtained starting from a Maxwellian distribution for the thermal velocity of molecules in thermodynamic equilibrium. In this case, it is possible to show that the following equation applies for the mass flow rate:

$$\dot{m} = \alpha p_0 \sqrt{\frac{m_a}{2\pi k T_0}} \cdot A_e \quad (5.8)$$

where  $m_a$  is the mass of a single molecule of gas,  $k$  is the Boltzmann constant, and  $A_e$  is the total exit area of all expansion slots. The parameter  $\alpha$  in Eq. (5.8), called transmission coefficient, is crucial in this type of system. It is defined as the actual mass flow rate of molecules expelled from the expansion slots, divided by the ideal mass flow rate in the free-molecular limit; or, in other words, the ratio of the mass flow rate of molecules actually exiting the expansion slots, to the mass flow rate of

molecules entering it. The two mass flow rates are not the same, as part of the molecules entering the expansion slots are bounced back and go back to the plenum without being expelled.

The transmission coefficient represents an important loss factor of LPM thrusters, as the molecules returning into the plenum, despite being partially energized in the expansion slot, are not expelled and therefore do not contribute to generating thrust. Semiempirical expressions for this coefficient can be found in Ref. [40], based on the geometry and shape of the expansion slot (in particular, for circular and rectangular ones). Typical values for expansion slots of constant area are in the range between 0.15 and 0.2, but it has been shown that they can be increased up to values higher than 0.7 with divergent expansion slots [34].

The jet velocity and exit pressure in a LPM system can then be written as follows:

$$v_e = \sqrt{\frac{\pi k T_{tr}}{2m_a}} \quad (5.9)$$

$$p_e = \frac{\alpha p_0}{\pi} \sqrt{\frac{T_{tr}}{T_0}} \quad (5.10)$$

where  $T_{tr}$  is the translational kinetic temperature of the gas, which depends on the specific heat ratio and wall temperature  $T_w$  in the expansion slot:

$$T_{tr} = \left( \frac{6\gamma}{\pi + 6\gamma} \right) T_w \quad (5.11)$$

Combining the above equations in the general expressions for the thrust and specific impulse, as given by Eqs. (5.3) and (5.4), it is finally possible to obtain the following expressions for the vacuum thrust ( $p_a = 0$ ) and the vacuum specific impulse:

$$F_{T\_vac} = \alpha p_0 A_e \frac{\pi + 2}{2\pi} \sqrt{\frac{T_w}{T_0} \left( \frac{6\gamma}{\pi + 6\gamma} \right)} \quad (5.12)$$

$$I_{sp\_vac} = \frac{\pi + 2}{g_0} \sqrt{\frac{k T_w}{2\pi m_a} \left( \frac{6\gamma}{\pi + 6\gamma} \right)} \quad (5.13)$$

Eqs. (5.12) and (5.13) confirm that, even in the very different fluid dynamic conditions of a LPM microthruster, similar considerations as in a conventional thruster based on continuum flow apply: the thrust level is proportional to the plenum pressure and the expansion slot area, while the specific impulse is mainly dependent on the wall temperature and the molecular mass. A noticeable difference is however that the wall temperature also influences in a direct way the thrust level, while it has an almost negligible effect on the thrust level of a conventional VLM microresistojet, see Eqs. (5.1) and (5.2) combined with Eq. (5.3). Finally, the transmission coefficient has direct influence on the thrust but does not affect directly the specific impulse.

## 5.5 Conclusion and future challenges

To better put in the right context electrothermal microthrusters, and more specifically microresistojets, it is possible to compare their current state-of-the-art performance with other types of micropropulsion systems. The information presented in Figs. 5.14–5.16 is based on data collected from various review papers [4,41–46] and provides an overview of the available micropropulsion alternatives in terms of thrust, specific impulse, input power, and thrust-to-power ratio.

From this comparison, it is clear that microresistojets offer the same versatility of cold gas thrusters in terms of their available range of thrust levels, but at better specific impulse (double to triple with respect to what is available with cold gas thrusters). This, of course, comes at the cost of the input electrical power required to heat the propellant.

While Fig. 5.14 clearly shows that microresistojets are still significantly far away in terms of specific impulse from other electric propulsion options and therefore not competitive with their propellant consumption efficiency, it can be clearly seen from Figs. 5.15 and 5.16 that microresistojets are by far the option with the highest thrust-to-power ratio, among those in which electrical power is needed to provide the required thrust energy to the propellant. This means that, although, with relatively poor propellant consumption efficiency, microresistojets are the option that allows for generating the highest thrust level with a given input power.

Concluding, the ideal application of miniaturized electrothermal thrusters is one in which versatility is an asset, both from the point of view of thrust and propellant

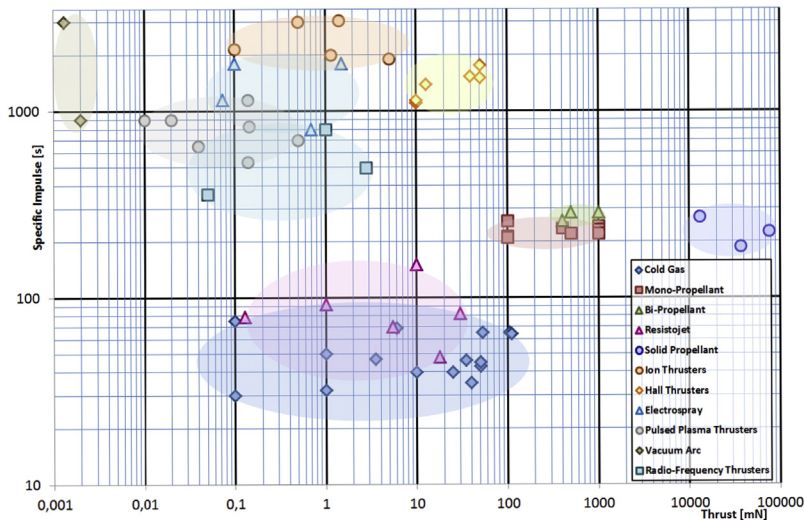
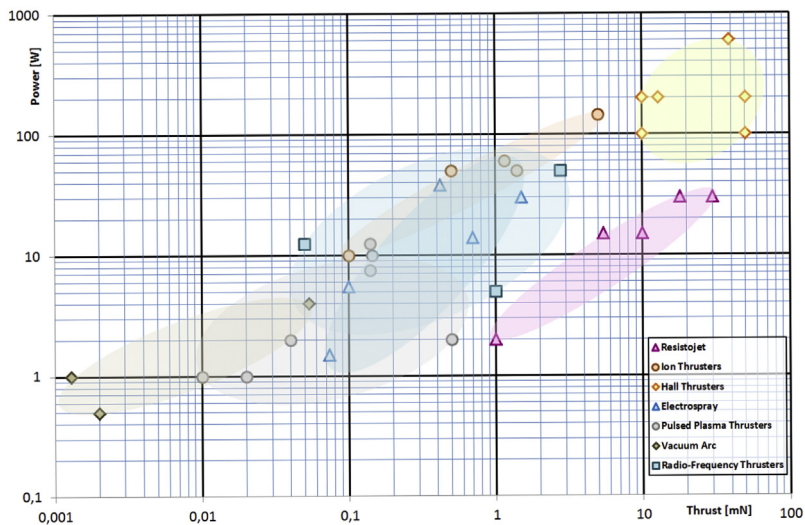


FIGURE 5.14

Current state of the art of various types of micropropulsion systems, in terms of thrust and specific impulse.



**FIGURE 5.15**

Current state of the art of various types of micropropulsion systems, in terms of thrust and input power.

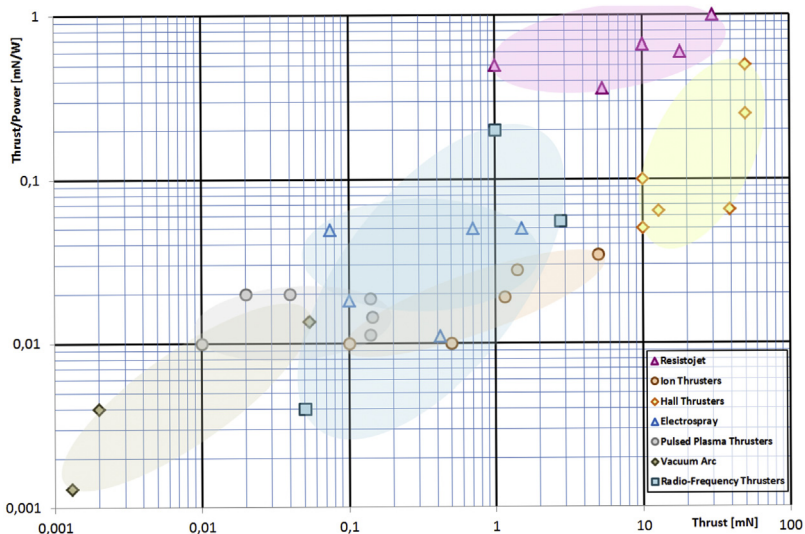


**FIGURE 5.16**

Current state of the art of various types of micropropulsion systems, in terms of thrust and thrust-to-power ratio.



choice. Whenever thrust levels in the order of 1–100 mN are required, in particular, microresistojets represent the only option that allows for achieving this thrust level with a power level of 10 W or lower (typical order of magnitude of the available average power in a small satellite such as a 3U CubeSat).

As it has been shown in this chapter, the state of the art of electrothermal micro-propulsion is extremely dynamic, with several options and concepts currently under development in universities, research centers, and companies.

The main advantage of this type of propulsion is its versatility, in particular the fact that it can be used with virtually any propellant in any state, solid, liquid, or gaseous.

In turn, the main challenges in the design of a conventional microresistojet thruster, where propellant is vaporized and subsequently accelerated in a convergent-divergent nozzle, are the flow instabilities and pressure oscillations intrinsically present in the two-phase flow in the heating chamber, with their consequences in terms of controllability of the thruster; the thermal efficiency of the propulsion system, intrinsically limited by the small size and the materials used; the flow losses in the nozzle, which can become significant at values of throat Reynolds number lower than 1000, which are typically obtained when the thrust level is in the mN range. These drawbacks can be partially overcome by considering alternative microresistojet concepts, such as the use of a separate vaporization chamber to reduce the issues generated by the two-phase flow, or the LPM option in which the low pressure and rarefied flow regime allow for making the conventional convergent-divergent nozzle not necessary anymore.

Generally speaking, miniaturized electrothermal propulsion presents interesting advantages that make it definitely worth further research, but is currently still at an embryonal stage. More developments in the field are certainly expected in the close future, with a concrete possibility for competitive technology being developed within the next 5–10 years.

---

## References

- [1] NASA Goddard Spaceflight Center, Vela 5A, <https://heasarc.gsfc.nasa.gov/docs/heasarc/missions/vela5a.html>.
- [2] Mickelsen, W.R., Isley, W.C., 1968. Auxiliary electric propulsion – status and prospects. In: Proceedings of the 5th Symposium on Advanced Propulsion Concepts.
- [3] Aerojet Rocketdyne, 2019. Electric Propulsion Systems. Available at: [www.rocket.com](http://www.rocket.com).
- [4] Lemmer, C., 2017. Propulsion for CubeSats. *Acta Astronaut.* 134, 231–243.
- [5] Palmer, K., Li, Z., Wu, S., 2016. In-orbit demonstration of a MEMS-based micro-propulsion system for CubeSats. In: Small Satellite Conference (Logan, Utah, USA).
- [6] Hejmanowski, N.J., et al., 2015. CubeSat high impulse propulsion system (CHIPS). In: Proceedings of the 62nd JANNAF Propulsion Meeting.
- [7] Hejmanowski, N.J., et al., 2015. CubeSat high impulse propulsion system (CHIPS) design and performance. In: Proceedings of the 63rd JANNAF Propulsion Meeting.

- [8] Hruby, V., 2012. High Isp CubeSat Propulsion, 1st Interplanetary CubeSat Workshop, Cambridge, MA, USA.
- [9] Moore, G., et al., 2010. 3D printing and MEMS propulsion for the RAMPART 2U CubeSat. In: Small Satellite Conference (Logan, Utah, USA).
- [10] Asakawa, J., et al., 2017. Development of the water resistojet propulsion system for deep space exploration by the CubeSat: EQUULEUS. In: Small Satellite Conference (Logan, Utah, USA).
- [11] Asakawa, J., et al., 2019. AQT-D: demonstration of the water resistojet propulsion system by the ISS-deployed CubeSat. In: Proceedings of the 33rd Annual AIAA/USU Conference on Small Satellites.
- [12] Koizumi, H., et al., 2019. Assessment of micropropulsion system unifying water ion thrusters and water resistojet thrusters. *J. Spacecraft Rockets* 56 (5), 1400–1408.
- [13] Maurya, D., et al., 2005. Silicon MEMS vaporizing liquid microthruster with internal microheater. *J. Micromech. Microeng.* 15 (5).
- [14] Kundu, P., et al., 2012. Design, fabrication and performance evaluation of a vaporizing liquid microthruster. *J. Micromech. Microeng.* 22 (2).
- [15] Ye, X., et al., 2001. Study of a vaporizing water microthruster. *Sensors Actuators A Phys.* 89 (1–2).
- [16] Mueller, J., et al., 1997. Design, analysis and fabrication of a vaporizing liquid microthruster. In: 33rd AIAA/ASME/SAE/ASEE Joint Propulsion Conference and Exhibit.
- [17] Mueller, J., et al., 1998. Proof-of-concept demonstration of a vaporizing liquid microthruster. In: 34th AIAA/ASME/SAE/ASEE Joint Propulsion Conference and Exhibit.
- [18] Mukerjee, E., et al., 2000. Vaporizing liquid microthruster. *Sensor. Actuator. A* 83 (1).
- [19] Silva, M.A.C., et al., 2017. Vaporizing liquid microthrusters with integrated heaters and temperature measurement. *Sensor. Actuator. A Phys.* 265.
- [20] Silva, M.A.C., et al., 2018. A comprehensive model for control of vaporizing liquid microthrusters. *IEEE Trans. Control Syst. Technol.* 99, 1–8.
- [21] Pallichadath, V., et al., 2019. In-orbit micro-propulsion demonstrator for pico-satellite applications. *Acta Astronaut.* 165, 414–423.
- [22] Karthikeyan, K., et al., 2012. Low temperature Co-fired ceramic vaporizing liquid microthruster for microspacecraft applications. *Appl. Energy* 97.
- [23] Cheah, K., et al., 2015. Fabrication and performance evaluation of a high temperature Co-fired ceramic vaporizing liquid microthruster. *J. Micromech. Microeng.* 25 (1).
- [24] Chen, C.C., et al., 2010. Simulation and experiment research on vaporizing liquid micro-thruster. *Sensor. Actuator. A Phys.* 157 (1).
- [25] Cen, J., et al., 2010. Performance evaluation and flow visualization of a MEMS based vaporizing liquid micro-thruster. *Acta Astronaut.* 67, 468–482.
- [26] De Giorgi, M.G., et al., 2019. A novel Quasi-one-dimensional model for performance estimation of a vaporizing liquid microthruster. *Aero. Sci. Technol.* 84, 1020–1034.
- [27] De Giorgi, M.G., et al., 2019. Preliminary evaluation of a MEMS-based water propellant vaporizing liquid microthruster for small satellites. In: XXV International Congress, Italian Association of Aeronautics and Astronautics.
- [28] Ketsdever, A., et al., 1998. A free molecule micro-resistojet: an interesting alternative to nozzle expansion. In: 34th AIAA/ASME/SAE/ASEE Joint Propulsion Conference and Exhibit.
- [29] Ketsdever, A., et al., 2001. Gas-surface interaction model influence on predicted performance of microelectromechanical system resistojet. *J. Thermophys. Heat Tran.* 15 (3), 302–307.

- [30] Ketsdever, A., et al., 2005. Performance testing of a microfabricated propulsion system for nanosatellite applications. *J. Micromech. Microeng.* 15 (2), 2254–2263.
- [31] Ahmed, Z., et al., 2005. Numerical analysis of free molecule micro-resistojet performance. *J. Propul. Power* 22 (4), 749–756.
- [32] Lee, R.H., et al., 2007. Performance characterization of free molecule micro-resistojet utilizing water propellant. In: 43rd AIAA/ASME/SAE/ASEE Joint Propulsion Conference and Exhibit.
- [33] Guerrieri, D.C., et al., 2017. Fabrication and characterization of low-pressure micro-resistojets with integrated heater and temperature measurement. *J. Micromech. Microeng.* 27, 12.
- [34] Guerrieri, D.C., 2016. Analysis of non-isothermal rarefied gas flow in diverging micro-channels for low pressure micro-resistojets. *ASME J. Heat Transfer* 138, 11.
- [35] Cervone, A., et al., 2015. Conceptual design of a low-pressure micro-resistojet based on a sublimating solid propellant. *Acta Astronaut.* 108, 30–39.
- [36] Leverone, F., et al., 2019. Cost analysis of solar thermal propulsion systems for micro-satellite applications. *Acta Astronaut.* 155, 90–110.
- [37] Kennedy, F.G., et al., 2002. Preliminary design of a micro-scale solar thermal propulsion system. In: 38th AIAA/ASME/SAE/ASEE Joint Propulsion Conference and Exhibit.
- [38] Sahara, H., et al., 2003. Single-crystal molybdenum solar thermal propulsion thruster. *Trans. Jpn. Soc. Aeronaut. Space Sci.* 46, 180–185.
- [39] Guerrieri, D.C., et al., 2017. Selection and characterization of green propellants for micro-resistojets. *ASME J. Heat Transfer* 139, 10.
- [40] Guerrieri, D.C., et al., 2018. An analytical model for characterizing the thrust performance of a low pressure micro-resistojet. *Acta Astronaut.* 152, 719–726.
- [41] Levchenko, I., et al., 2018. Space micropropulsion systems for cubesats and small satellites: from proximate targets to furthestmost frontiers. *Appl. Phys. Rev.* 5 (1).
- [42] Tummala, A.R., et al., 2017. An overview of cube-satellite propulsion technologies and trends. *Aerospace* 4 (4), 58.
- [43] Krejci, D., et al., 2018. Space propulsion technology for small spacecraft. *Proc. IEEE* 106 (3), 362–378.
- [44] Silva, M.A.C., et al., 2018. A review of MEMS micropropulsion technologies for CubeSats and PocketQubes. *Acta Astronaut.* 143, 234–243.
- [45] Parker, K.I., 2016. State-of-the-Art for small satellite propulsion systems. In: Proceedings of the 4th NSBE Aerospace Systems Conference.
- [46] Leomanni, M., et al., 2017. Propulsion options for very low Earth orbit microsattelites. *Acta Astronaut.* 133, 444–454.

---

## Further reading

- [1] Sutton, G.P., Biblarz, O., 2001. *Rocket Propulsion Elements*, seventh ed. John Wiley & Sons.